

# Biom mineralization markers during early shell formation in the European abalone *Haliotis tuberculata*, Linnaeus

Béatrice Gaume · Martine Fouchereau-Peron ·  
Aïcha Badou · Marie-Noëlle Helléouet ·  
Sylvain Huchette · Stéphanie Auzoux-Bordenave

Received: 12 May 2010 / Accepted: 5 October 2010 / Published online: 26 October 2010  
© Springer-Verlag 2010

**Abstract** Larval shell formation was investigated in the European abalone *Haliotis tuberculata*. Stages of mineralization as well as enzymatic and endocrine biomarkers were monitored throughout larval development, from hatching to post-larval stages. Polarized light microscopy and infrared spectroscopy analyses revealed the presence of crystallized calcium carbonate arranged in aragonite polymorphs from the late trochophore stage. A correlation between the main steps of shell formation and enzymatic activities of alkaline phosphatase and carbonic anhydrase was seen. The variations of these biologic activities were related to the onset of mineralization, the rapid shell growth, and the switch from larval to juvenile shell following metamorphosis. Furthermore, a strong increase in the level of calcitonin gene-related molecules was measured in post-larvae, suggesting that endocrine control

takes place after metamorphosis. The changes measured for the three biom mineralization markers together with mineralogical analysis allowed us to correlate physiologic mechanisms with early steps of abalone shell formation.

## Introduction

The molluskan shell is an organo-mineral bioceramic structure exhibiting a large array of shapes and microstructures among members of this phylum. The combination of  $\text{CaCO}_3$ —crystallized in either calcite or aragonite polymorphs—with an organic matrix enhances the mechanical properties of the shell providing a highly rigid protection to the soft tissues (Watabe 1988; Wilbur and Saleuddin 1983). When observed in cross-section, the shell shows a succession of three overlapping layers: an external periostracum (organic), a prismatic layer (calcite/aragonite), and an internal nacreous layer (aragonite) each of them being controlled by specific nucleating or inhibiting proteins (Belcher et al. 1996; Falini et al. 1996; Lowenstam and Weiner 1989; Marin and Luquet 2004). Although the structure and formation of adult shell has been well documented (Dauphin et al. 1989; Mutvei et al. 1985), few studies were set about the early shell formation (see Kniprath 1981; for review). Furthermore, the biochemical and molecular mechanisms underlying larval shell formation remain largely unknown (Jackson et al. 2007).

In Gastropods, the shell forms initially during embryonic development with the formation of the shell gland that secretes the periostracum. Then, the shell gland everts to give rise to the shell field, which will form the calcifying mantle (Jablonski and Lutz 1980). The bordering epithelial cells produce a fine organic layer from which the first larval organic shell called the protoconch I originates. In the early

---

Communicated by H. O. Pörtner.

---

B. Gaume (✉) · M. Fouchereau-Peron · M.-N. Helléouet ·  
S. Auzoux-Bordenave  
UMR BOREA (Biologie des Organismes et Ecosystèmes  
Aquatiques), MNHN/CNRS 7208/IRD 207/UPMC,  
Muséum national d'Histoire naturelle,  
Station de Biologie Marine, 29900 Concarneau, France  
e-mail: bordenav@mnhn.fr

A. Badou  
UMR 7194/USM 204, Centre de Spectroscopie Infrarouge,  
Département Préhistoire, Muséum National d'Histoire Naturelle,  
43 rue Buffon, 75005 Paris, France

S. Huchette  
Ecloserie France-Haliotis, Kérazan, 29880 Plouguerneau, France

S. Auzoux-Bordenave  
Université Pierre et Marie Curie Paris VI,  
4 place Jussieu, 75005 Paris, France

pre-torsional veliger stage, the larval mantle starts to drive  $\text{CaCO}_3$  precipitation through the synthesis and secretion of organic components (Crofts 1937; Jackson et al. 2007; Kniprath 1981; Marin et al. 2007; Page 1997). In larval abalone, it has been shown that mineralization occurs at this stage and that the mineral phase initially deposited is mostly composed of aragonite (Jardillier et al. 2008). Protoconch I enlarges to become protoconch II that achieves its growth just after the  $180^\circ$  torsion. At metamorphosis, protoconch II gives support to the future juvenile shell formation and is then fully integrated in the adult shell.

Shell biomineralization involves the uptake of mineral ions from the environment and their precipitation into  $\text{CaCO}_3$  controlled by an organic matrix secreted by specialized cells of the outer mantle epithelium. The extrapallial area, located between the mantle and the inner shell, is the preferential site for biomineralization as this is where organic components interact with bicarbonate and calcium ions to form crystallized  $\text{CaCO}_3$  (Lin and Meyers 2005; Watabe 1988; Wilbur and Saleuddin 1983). The calcifying matrix, which accounts for 0.1 to 5% of the shell, is a mixture of proteins, glycoproteins, lipids, chitin, and acidic polysaccharides that drives crystal nucleation, selects the  $\text{CaCO}_3$  polymorph, and controls the growth and spatial arrangement of minerals (Falini et al. 1996; Levi-Kalishman et al. 2001). Among this organic complex network controlling the mineralization process, some enzymes are involved in matrix component maturation and in accelerating ion precipitation (Weiss and Marin 2008).

Alkaline phosphatase (AP) is a ubiquitous enzyme involved in biomineralization in vertebrates. In mammals, the tissue-non-specific alkaline phosphatase (TNAP) is expressed in bones and is used as a marker for osteoblast maturation (Almeida et al. 2000). In mollusks, AP activity has been reported in the mantle epithelium and in the larval shell field (Bevelander and Benzer 1948; Bielefeld and Becker 1991; Marxen et al. 2003; Timmermans 1969). AP has been localized in both internal and external mantle epithelium and in hemolymphatic lacunae of the abalone *Haliotis tuberculata* (Bielefeld and Becker 1991; Blasco et al. 1993). Significant AP activity variations during adult shell growth were related to the biomineralization process (Blasco et al. 1993; Duvail and Fouchereau-Peron 2001). These results strongly suggest a role of AP in the regulation of molluskan shell mineralization. However, the precise role of the enzyme in shell calcification still needs to be clarified.

Another important enzyme implicated in both the respiration and biomineralization processes is carbonic anhydrase (CA), which catalyzes the reversible hydration of carbon dioxide to form bicarbonate ions  $\text{HCO}_3^-$ . Carbonic anhydrase was identified in the mantle and gills

of many mollusks and has long been linked with shell formation (Freeman and Wilbur 1948). The direct role of CA in the rapid growth of molluskan shell was first demonstrated in the oyster *Crassostrea gigas* (Wilbur and Jodrey 1956) and confirmed in a fresh-water snail by specific inhibition experiments (Freeman 1960). In marine bivalves, CA activity is found to be correlated with the main steps of larval shell development and the onset of biomineralization (Medakovic 2000). Enzymatic variations were also measured during the abalone growth with an increased activity observed in gills (Duvail and Fouchereau-Peron 2001). The most obvious role suggested for CA is the acceleration of bicarbonates ions formation for  $\text{CaCO}_3$  precipitation.

The temporal and spatial variations observed in the calcifying activity over molluskan development and the drastic switch in the mineralizing program observed at metamorphosis suggest an endocrine control of shell formation (Joosse 1988). Calcitonin gene-related peptides (CGRP), derived from the alternative splicing of a common primary calcitonin transcript (Amara et al. 1982), are known to control calcium metabolism (Tippins et al. 1984) and stimulate osteoblast proliferation in vertebrates (Vignery and McCarthy 1996). In marine mollusks, CGRP-like molecules have been found in mantle and gills (Duvail et al. 1997), but their role in the biomineralization process still needs to be clarified. In the oyster *Pinctada margaritifera*, a hypocalcemic role of CGRP-like molecules has been demonstrated (Rousseau et al. 2003). In vitro, it is shown that human CGRP increases CA activity in abalone hemocytes and mantle cells (Auzoux-Bordenave et al. 2007) and also stimulates CA activity in *Pinctada margaritifera* gill membranes via a CT/CGRP common receptor (Cudennec et al. 2006). Thus, CGRP-like molecules may likely control the biomineralization process through the activation of CA activity and a hypocalcemic effect.

The present study was undertaken to further understand the biochemical control of early shell formation and to link the mineralization sequence with biologic processes during the shell morphogenesis. Combined polarized light microscopy, specific calcium staining, and FTIR spectroscopy were used to follow early steps formation and to determine the onset of mineralization in *Haliotis tuberculata* larvae. The presence and activity of three biomineralization markers were investigated in the same developmental stages of the abalone. Both the activities of carbonic anhydrase and alkaline phosphatase enzymes and the levels of CGRP-like molecules were measured from early trochophore to post-larval stages. The results allow the relation of the variations of biochemical markers with the main steps of early abalone shell mineralization.

## Materials and methods

### Animals

*H. tuberculata* (Linnaeus) larvae and post-larvae (about 60,000 per stage) were obtained from controlled fertilizations held at the French hatchery France-Haliotis (S. Huchette, Plouguezeau, France) in July 2008 at a water temperature of  $19^{\circ}\text{C} \pm 0.5^{\circ}\text{C}$ . The timing of larval development with the main steps of shell morphogenesis is shown in Fig. 1. Fertilization occurs in sea water and originates a spherical egg. About 16 h post-fertilization, a trochophore larva hatches from the egg membrane with a characteristic spinning-top shape. The first larval shell, the protoconch I, is detected 19 h post-fertilization on the post-lateral side. In the pre-torsional veliger stage (25 hpf), larva acquires a velum. The foot and the mantle begin to differentiate as the larval shell, the protoconch II, enlarges to surround the body. The larva undergoes a  $180^{\circ}$  torsion so that the mantle cavity and gills are twisted into the shell, opposite the foot. In the post-torsional veliger stage (51 hpf), the larva can withdraw inside the shell. Just before metamorphosis (94 hpf), the eyes are formed and the mantle covers the entire dorsal part of the

larva. After 4 to 5 days of pelagic life, the larva loses the velum, begins to settle down and starts metamorphosis to become a benthic post-larva. After metamorphosis, the 6–7 day-old post-larva exhibits the transition between protoconch and newly deposited juvenile shell. Fresh, live larvae at different developmental stages were filtered on a  $40\text{-}\mu\text{m}$  sieve. Then, larvae were immediately fixed for microscopic observations and FTIR, or frozen in liquid nitrogen for enzymatic analyses and radioimmunoassay.

For adult tissue analyses, five 7-cm-length abalone from the hatchery were used. Animals were grown in open sea and fed with handpicked fresh seaweed. They were collected in March and dissected at the hatchery. Mantle and gills were immediately frozen in liquid nitrogen for further enzymatic analyses.

### Histology

About 3,000 larvae from different developmental stages were fixed at room temperature for 2 h with 3% paraformaldehyde diluted in phosphate-buffered saline (PBS: 137 mM NaCl, 3 mM KCl, 10 mM  $\text{Na}_2\text{HPO}_4$ , 2 mM  $\text{KH}_2\text{PO}_4$ ). After fixation, the larvae were rinsed 3 times in

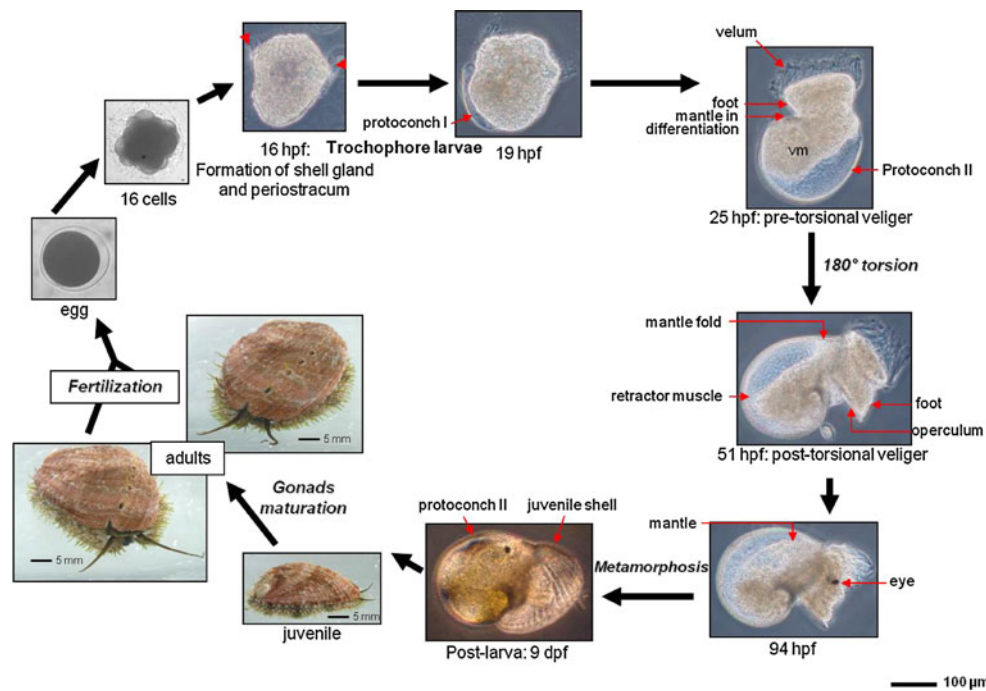


**Fig. 1** Life cycle of the abalone *Haliotis tuberculata* at  $19^{\circ}\text{C} \pm 0.5^{\circ}\text{C}$ . Larval stages were observed by phase contrast microscopy and obtained from controlled fertilizations held at the hatchery France-Haliotis. Fertilization originates a spherical egg. It undergoes successive divisions to form 4, 8, and 16 cell embryo. About 16 h post-fertilization, a trochophore larva hatches from the egg membrane with a prototroch ciliary band (arrows). The first larval shell, the protoconch I, is detected 19 h post-fertilization in the post-lateral side. The pre-torsional veliger stage (25 hpf) acquires a velum

and the larval shell, the protoconch II, enlarges to surround the body. The larva then undergoes a  $180^{\circ}$  torsion. In the post-torsional veliger stage (51 hpf), the larva can withdraw inside the shell which is closed by the operculum. Just before metamorphosis (94 hpf), the mantle covers the entire dorsal part of the larva. After metamorphosis, the 6–7 day-old post-larva exhibits a sharply defined transition between protoconch and newly deposited juvenile shell, the latter showing the typical ornamentations of the adult shell. hpf: hours post-fertilization, vm: visceral mass, dpf: days post-fertilization

a 0.01 M PBS (pH 7.4) and stored in 70% ethanol at 4°C until dehydration. A double inclusion in agar–agar and paraffin (Paraplast<sup>®</sup>, Sigma–Aldrich) was made to embed about ten larvae per stage. Embedded samples were cut in 5–6- $\mu$ m sections with an American Optical microtome (Spencer 820 type). After removing paraffin and rehydration, the slides were stained with 2% alizarin red for 2 min to localize calcium deposits (Martoja and Martoja 1967). The slides were mounted with a hydrophobic medium (Eukitt<sup>®</sup>, Sigma–Aldrich) and observed with an Olympus binocular microscope BX51 (Olympus, Hamburg, Germany).

#### Light polarized microscopy

About ten larvae per stage were whole-mounted between glass slide and cover-slip in a drop of glycerol/PBS. Preparations were observed by phase contrast microscopy and light polarized microscopy with an Olympus binocular microscope. All polarized images were acquired at maximum light source with a high-definition color camera (DS-Ri1, Nikon).

#### Fourier transform infrared spectroscopy (FTIR)

Larvae were fixed in 50% ethanol/PBS at the hatchery and dehydrated by successive ethanol baths. Ethanol was then evaporated in a drying oven at 50°C over 5 h. Larvae were weighed and about 0.2 mg was pressed in 300 mg of potassium bromide (KBr). The powdered samples were pressed in KBr pellets according to the method already described (Fröhlich and Gendron-Badou 2002; Pichard and Fröhlich 1986). Pellets were examined using a Fourier Transform Infrared (FTIR) spectrometer (Bruker-Vector 22) over a range from 2,000 to 400  $\text{cm}^{-1}$ . The analysis was performed at 2  $\text{cm}^{-1}$  resolution and accumulation of 32 scans. A background spectrum was measured for pure KBr.

#### Extraction procedure for enzymatic activity assay

Adult tissues and whole larval samples (about 50,000 larvae per stage) were immediately frozen in liquid nitrogen at the hatchery and stored at  $-80^{\circ}\text{C}$  until use. Samples were maintained in ice over all the extraction procedure. They were weighed and homogenized in 6 volumes of 125 mM PBS (pH 7.4) using an Ultra Turrax grinder. After centrifugation at 1,000 g for 5 min at 4°C, supernatants were filtered through a 200- $\mu$ m sieve and stored at  $-80^{\circ}\text{C}$  until use.

#### Alkaline phosphatase activity

Alkaline phosphatase activity was measured according to the colorimetric method from Bourgoin et al. 1996. Each

extract (adult tissues or whole larval samples) was diluted in alkaline buffer (Sigma–Aldrich) to obtain a total protein concentration of 300  $\mu\text{g}/\text{ml}$  and 100  $\mu\text{l}$  of each dilution were deposited on a 96-well plate. A volume of 100  $\mu\text{l}$  of p-NitroPhenol Phosphate (Sigma–Aldrich) was added to each well. The plate was incubated for 1 h at 37°C, and the reaction was stopped with the addition of 50  $\mu\text{l}$  of 3 M NaOH. Absorbances were measured at 405 nm with a BioRad microplate reader. A standard curve was made with p-NitroPhenol (Sigma–Aldrich) at concentrations ranging from 3.9 to 62.5 nmol/ml.

#### Carbonic anhydrase activity

Total carbonic anhydrase activity was measured using the  $\Delta\text{pH}$  method (Vitale et al. 1999). The reaction medium was composed of mannitol (225 mM), sucrose (75 mM) and Tris–phosphate (10 mM), the pH being adjusted to 7.4 with ortho-phosphoric acid (20 mM). For each measurement, 7.5 ml of the reaction medium and 1 ml of  $\text{CO}_2$  saturated ice-cold distilled water were mixed with 500  $\mu\text{l}$  of larval or tissue extracts (equivalent to 300  $\mu\text{g}$  of total proteins). The pH decrease was recorded within 100 s with a pH meter (HI 931401, Hanna Instruments) connected to a computer. The linear regression was adjusted to pH data versus time. The slopes represent the catalyzed reaction rate ( $b_c$ ). The non-catalyzed reaction rate ( $b_{nc}$ ) was estimated from the pH drop of the control, without larval or tissue extract. The specific carbonic anhydrase activity was calculated with the following formula ( $b_c/b_{nc}-1$ )/mg of proteins. Carbonic anhydrase activity was also measured in the presence of 30  $\mu\text{M}$  acetazolamide (diluted in DMSO), a specific inhibitor of the enzyme.

#### CGRP radioimmunoassay

Larval and tissue extracts were homogenized in 10 volumes of 0.1 N acetic acid using an UltraTurrax homogenizer. Samples were boiled for 10 min. After centrifugation (1,800 g, 20 min), the supernatant was filtered, freeze-dried, and stored at  $-20^{\circ}\text{C}$  until assayed. The radioimmunoassay was performed according to the method already described (Fouchereau-Peron 1993). An antihuman CGRP antibody (gift from Dr. A. Julienne U349 INSERM, Paris, France) at a final dilution of 1/175 000, was incubated with serial dilutions of standard hormone (type I human CGRP from Bachem (Merseyside, UK) or larval extracts, overnight at 30°C. Then, the  $^{125}\text{I}$ -hCGRP (Perkin-Elmer, 2,000 Ci/mmol) was added and the samples were incubated at 4°C for 21 h. The separation of bound and free hormones was made by a charcoal–dextran precipitation. Results are expressed as the percentage of maximal binding ( $B_0$ ), where  $B_0$  represents the binding of labeled peptide in the absence of unlabeled hormone. Linearization of the

standard curves was carried out by plotting  $\ln[(B/B_0)/1 - (B/B_0)]$  (logit) as a function of  $\ln$  of hormone concentration. Each larval extract was serially diluted. The dose–response curves were statistically compared to the standard curve in order to estimate their parallelism.

#### Protein concentration

Total protein concentration in larval and tissue extracts were quantified using the bicinchoninic acid protein assay (BCA, Interchim) under the conditions described by the manufacturer. Bovine Serum Albumin (BSA, Sigma–Aldrich) was used as a standard at concentrations ranging from 10 to 100  $\mu\text{g/ml}$ .

#### Statistical analyses

Statistical analyses were performed with the software Statgraphics (Statpoint Technologies, Warrenton, Virginia, USA). All data are shown as means  $\pm$  s.e.m. Differences between groups were assessed by the Student's *t* test, and a probability of  $P < 0.05$  was considered to be statistically significant.

## Results

### Larval shell mineralization

Polarized light microscopy and alizarin red staining were assayed on several stages from hatching to metamorphosis, to monitor shell formation and mineralization over the larval development of the abalone *H. tuberculata* (Fig. 2).

At the hatching stage (16 hpf), the spinning-top shaped larva revealed no birefringence under polarized light (Fig. 2a). Birefringence was observed from the late trochophore stage (19 hpf). The signal was a faint brightness in the post-lateral part of the larva (Fig. 2c) which corresponded to the position of the first larval shell observed during development (Fig. 1, 19 hpf). Under identical observation conditions, veliger stages displayed a more intense birefringence (Fig. 2e, g) as the shell enlarged to surround the body. After larval torsion, shell birefringence increased and extended to the whole shell surface (Fig. 2i, k).

Alizarin red staining was used to detect calcium deposits in the growing shell. A red coloration was first detected in the shell area of the late trochophore stage at 19 hpf (Fig. 2d). In the following stages, alizarin staining was always restricted to the protoconch area with an increasing intensity as shell grew (Fig. 2d, f, h, j and l).

To ensure that birefringence observed from 19-h-old trochophore was due to a crystal lattice, the same stages were analyzed by infrared spectroscopy. IR spectra are

presented in Fig. 3. At the hatching stage (16 hpf), bands observed at 879, 1,048, and 1,454  $\text{cm}^{-1}$  were attributed to calcium carbonate vibrations. The absence of any band at 712  $\text{cm}^{-1}$  indicated that  $\text{CaCO}_3$  was not crystallized into a distinct polymorph and may likely correspond to amorphous calcium carbonate (ACC). From 19 hpf trochophore stage, larval spectra exhibited characteristic aragonite bands with the doublet at 700–712  $\text{cm}^{-1}$  associated with carbonate vibrations at 856, 1,082 and 1,470  $\text{cm}^{-1}$ . As larvae were analyzed in toto, the others bands observed on spectra, particularly after 1,500  $\text{cm}^{-1}$  are likely to be related to organic matter.

### Alkaline phosphatase activity

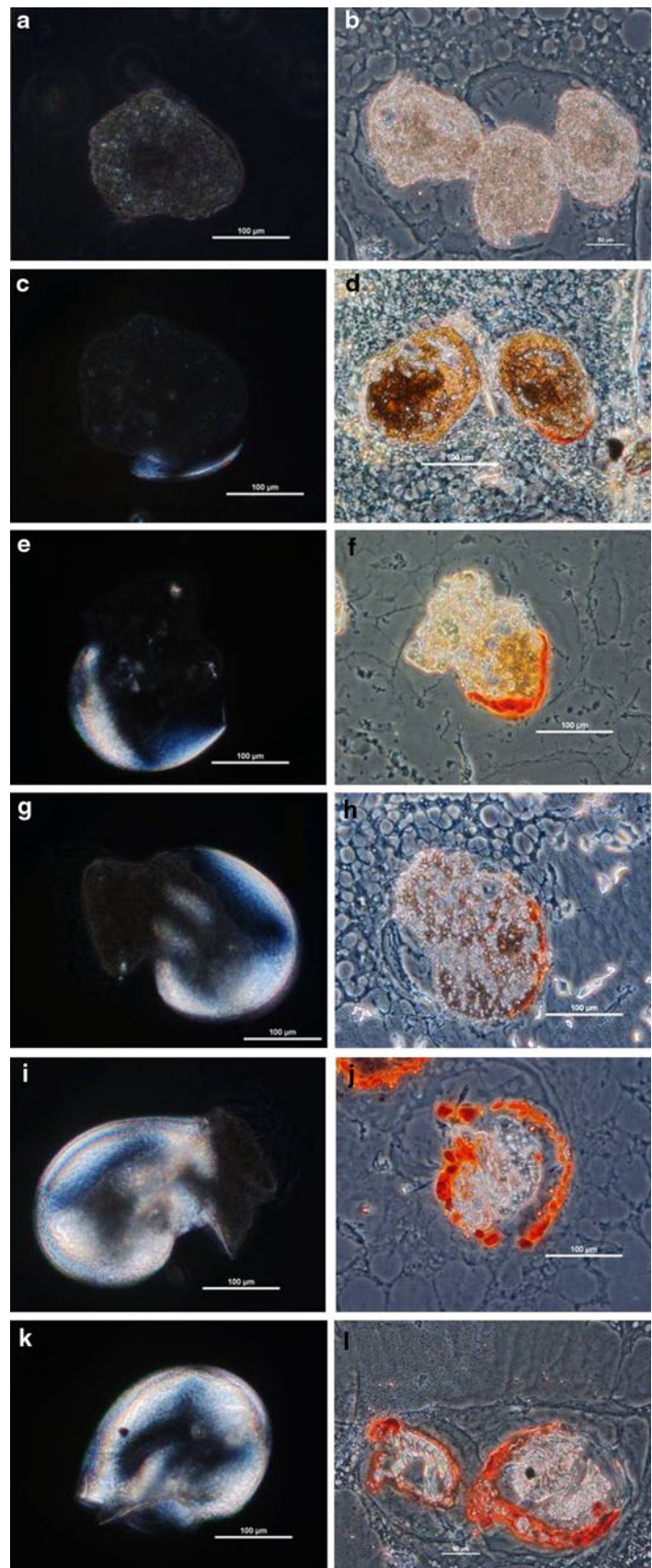
The activity of AP was assayed in the mantle of 7-cm-length abalone sampled in March, at the beginning of the annual shell growth period. In the mantle, the mean activity was 443 U/mg proteins (Fig. 4).

AP activity was measured along larval development in 3 sample series collected in 2006, 2007, and 2008. As the same trend was observed for the three series, only results from the 2008 sampling are presented in Fig. 4. Significant variations were observed during larval development. At hatching stage (16 hpf), the activity was 520 U/mg proteins. A significant decrease was observed between 16 and 28 hpf with a minimum at 330 U/mg proteins. At 45 and 69 hpf, two significant increases were observed with an activity of about 610 U/mg proteins. Between these two peaks, the activity was maintained close to that observed at the hatching stage (16 hpf). Just before metamorphosis, the AP activity peaked at 1,730 U/mg of proteins (93 hpf) and then dropped to 710 U/mg of proteins (96 hpf). After metamorphosis, a slight increase was observed again in 7-day-old post-larvae up to 835 U/mg proteins.

### Carbonic anhydrase activity

The specificity of the pH decrease method was tested by measuring human carbonic anhydrase II (hCA) activity with and without 30  $\mu\text{M}$  acetazolamide, a specific inhibitor of the enzyme. Adult abalone tissues and larvae were also assayed with and without the specific inhibitor at the same concentration (Fig. 5). The activity measured for 1  $\mu\text{g/ml}$  hCA was  $1,690 \pm 520$  U/mg proteins and a 100% inhibition of CA activity was observed in the presence of acetazolamide. In abalone tissues, the inhibition was respectively about 88% for mantle, 92% for gills and 70% for larvae thus evidencing the specificity of the method used. CA activity measured in gills was 1.7 times higher than in the mantle with 1,920 mU/mg proteins and 1,150 mU/mg proteins, respectively.

**Fig. 2** Larval stages in the development of *Haliotis tuberculata* showing progressive shell mineralization. Larvae were observed in toto by polarized light microscopy (*left column*). Histologic sections were stained with alizarin red and observed by phase contrast microscopy (*right column*). **a**, **b** newly hatched trochophore larvae, 16 hpf; **c**, **d** trochophore larvae, 19 hpf; **e**, **f** pre-torsional veliger, 22 hpf; **g**, **h** pre-torsional veliger, 25 hpf; **i**, **j** post-torsional veliger, 51 hpf; **k**, **l** late veliger stage, 69 hpf



Carbonic anhydrase activity was measured throughout larval development of the abalone (Fig. 6). In early larval stages, an exponential increase was observed from 16 hpf ( $453 \pm 122$  mU/mg proteins) to 28 hpf with  $1160 \pm 30$  mU/mg proteins (Fig. 6). Between 28 and 73 hpf, CA activity remained at a high level, about 2.6 higher than that measured at the hatching stage (16 hpf). Just before metamorphosis, the activity dropped around 600 mU/mg proteins and remained relatively stable in 6, 7, and 9-day-old post-larvae. A slight decrease was observed at 10 days post-fertilization.

#### Quantification of CGRP-like molecules

The effect of different concentrations of larval extract on the binding of  $^{125}\text{I}$ -CGRP to its antibody was tested by RIA and compared to the effect obtained with increasing dilutions of human CGRP (Fig. 7). Larval extracts inhibited the maximal binding of  $^{125}\text{I}$ -CGRP to its antibody as a function of protein concentration. 50% of inhibition was observed with 442  $\mu\text{g}$  of larval extract protein. As no significant difference was observed between regression lines—slopes were  $-0.9416$  and  $-0.786$  for hCGRP and larval extract, respectively—CGRP-like molecules were quantified in larval extracts using hCGRP as a standard reference.

The presence of immunoreactive CGRP-like (ir-CGRP) molecules was assessed in different developmental stages of *H. tuberculata* (Fig. 8). The level of CGRP-like molecules remained relatively stable during larval development, around 250 pg/mg proteins, until metamorphosis that takes place between 120 and 168 hpf. A slight increase was observed in post-torsional veliger stages, from 72 to 120 hpf, with about 350 pg of ir-CGRP/mg of proteins. After metamorphosis, from 7 days post-fertilization, the level of CGRP-like molecules was about threefold higher than in pre-metamorphic stages.

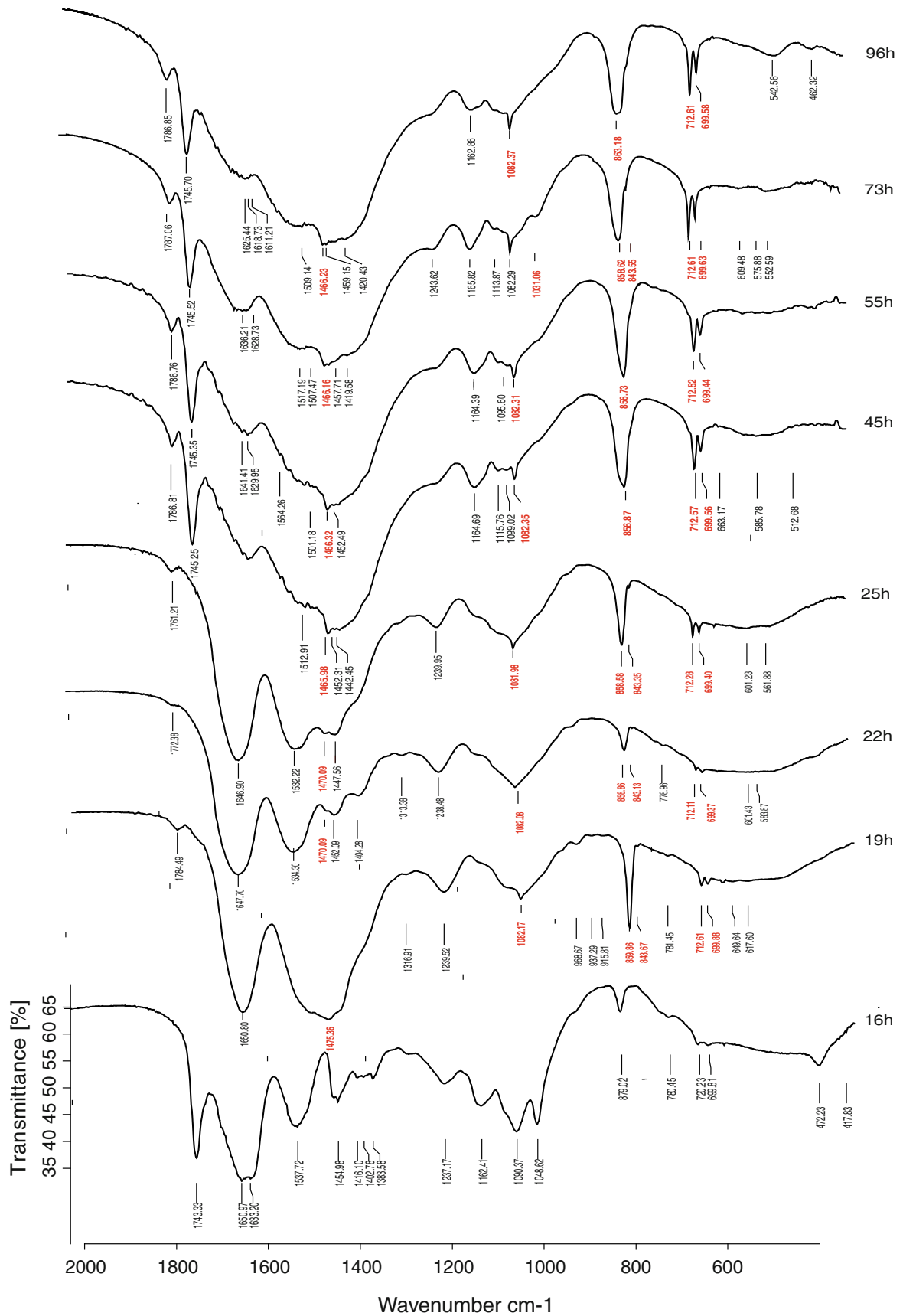
#### Discussion

This work has determined for the first time a succession of enzymatic activation/inhibition and variations of CGRP-like molecules, which are correlated to the main stages of abalone shell morphogenesis. The main results are summarized in Fig. 9, which correlate physiologic mechanisms to larval shell formation.

Mineralization of larval shell was investigated by calcium staining, polarized microscopy, and infrared spectroscopy. The alizarin staining of histologic sections reveals the presence of calcium deposits in the post-lateral area of the larvae corresponding to the protoconch I (19 hpf). The intensity of coloration increases throughout the larval development revealing an accumulation of

calcium carbonate in the shell. Cross-polarization observations show an increase of birefringence from early trochophore (19 hpf) to late veliger (69 hpf), confirming that larval shell contains more and more crystallized  $\text{CaCO}_3$ , as previously observed in the growing abalone shell (Jardillier et al. 2008). These results are in accordance with the observations of a calcified protoconch at an equivalent trochophore stage in *Haliotis asinina* (Jackson et al. 2007). In addition, infrared analysis confirms that early protoconch is mostly composed of ACC (amorphous calcium carbonate) that is transformed after few hours into crystalline aragonite. In a previous study, the first signal of aragonite deposition in abalone protoconch occurred around 30 hpf (Jardillier et al. 2008). This time-lag in shell mineralization could be explained by a difference in seawater temperature between the two sampling periods (respectively  $17^\circ\text{C}$  in 2005 and  $19 \pm 0.5^\circ\text{C}$  in 2008). As temperature is known to affect the timing of development in invertebrates (Bevelander 1988), the  $2^\circ\text{C}$  temperature increase in the 2008 series results in an accelerated development, therefore inducing a precocious shell formation. Furthermore, in the present study, the time-spaced sampling is adjusted to 3 h in order to cover more precisely the early stages of shell morphogenesis (compared to the 8-h-spaced sampling in our previous study). Our microscopic and mineralogic analyses confirm that abalone shell mineralization occurs at an early larval stage with crystallized calcium carbonate arranged in aragonite polymorphs.

To understand further the physiologic mechanisms involved in early shell formation, the activities of two biomineralizing enzymes, carbonic anhydrase and alkaline phosphatase, were measured from the early trochophore to post-larval abalones and compared to that in adult mantle. The mean AP activity measured in the first 3 days of larval development is similar to the one found in adult mantle during active shell growth (Duvail and Fouchereau-Peron 2001). AP activity is detected from an early trochophore stage (16 hpf) which corresponds to the shell field and periostracum formation (Fig. 9). This observation is consistent with AP activity found in the shell field of the freshwater gastropod *Biomphalaria glabrata* at an embryonic stage (Marxen et al. 2003). Furthermore, our results show that the maximum AP activity is reached just before metamorphosis, when larvae undergo drastic anatomic and physiologic changes to become benthic post-larvae. Thus, maximum AP activities can be found before protoconch and juvenile shell mineralization. These results confirm a role of AP in the initiation of mineralization but not in mineralization itself, as previously observed in vertebrates (Genge et al. 1988). Moreover, it has been suggested that AP could help in matrix protein maturation by acting like a phosphoprotein phosphatase (Lau et al. 1985; Marxen et al. 2003; Tsujii 1976). Thus, we can hypothesize a maturation



◀ **Fig. 3** FTIR spectra of larval shell from 16, 19, 22, 25, 45, 55, 73, and 96 h post-fertilization (hpf) stages. *Haliotis tuberculata* larval samples were ground and mixed with KBr. The mixture was pressed into a 7-mm-diameter pellet under vacuum and analyzed at 2 cm<sup>-1</sup> resolution with a Fourier Transform Infrared (FTIR) spectrometer (Bruker-Vector 22). Peaks at 879, 1,048, and 1,454 cm<sup>-1</sup> in 16 hpf stage indicate CaCO<sub>3</sub> vibrations. From 19 hpf, the appearance of the doublet at 700–712 cm<sup>-1</sup> reveal the CaCO<sub>3</sub> crystallization into aragonite

of organic matrix proteins by AP in the shell field and during secretome switch before juvenile shell formation.

Carbonic anhydrase activity, the main enzyme known to be involved in mollusk shell biomineralization, was also measured in larval and adult abalone. The mean CA activity in larvae is about 75% of activity measured in mantle of 7-cm-length abalone. During the first day of

**Fig. 4** Alkaline phosphatase activity during larval development. Each point represents the mean ± s.e.m. of four values. The experiments were carried out 3 times on a same pool of about 15,000 larvae collected in 2008. The same trend was observed for larvae collected in 2007 and 2006. AP activity measured in mantle of a 7-cm-abalone is reported in dotted line. Results are expressed in Units of activity per mg of total proteins in the larval extract. The letters, when different, indicate a significant difference between stages (*P* < 0.01). dpf: days post-fertilization

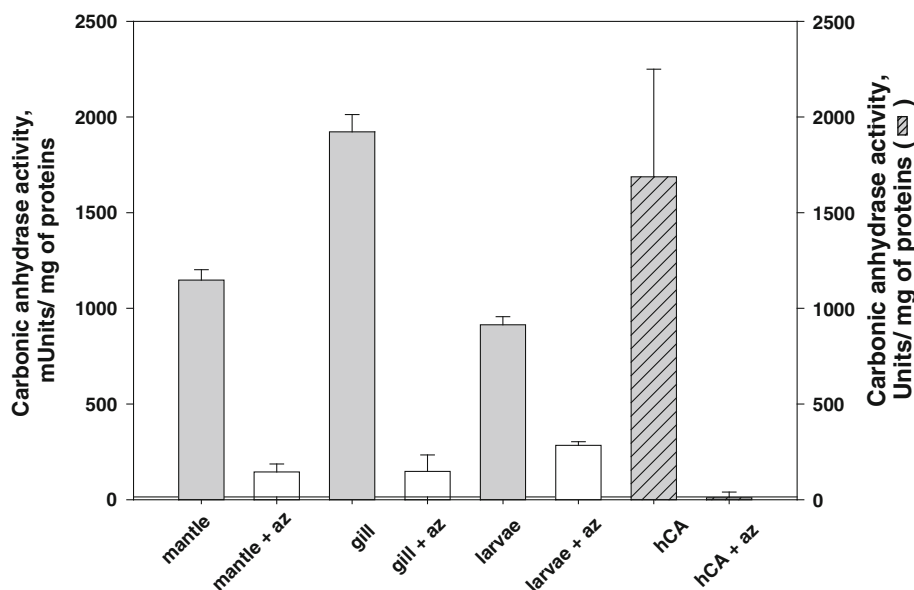
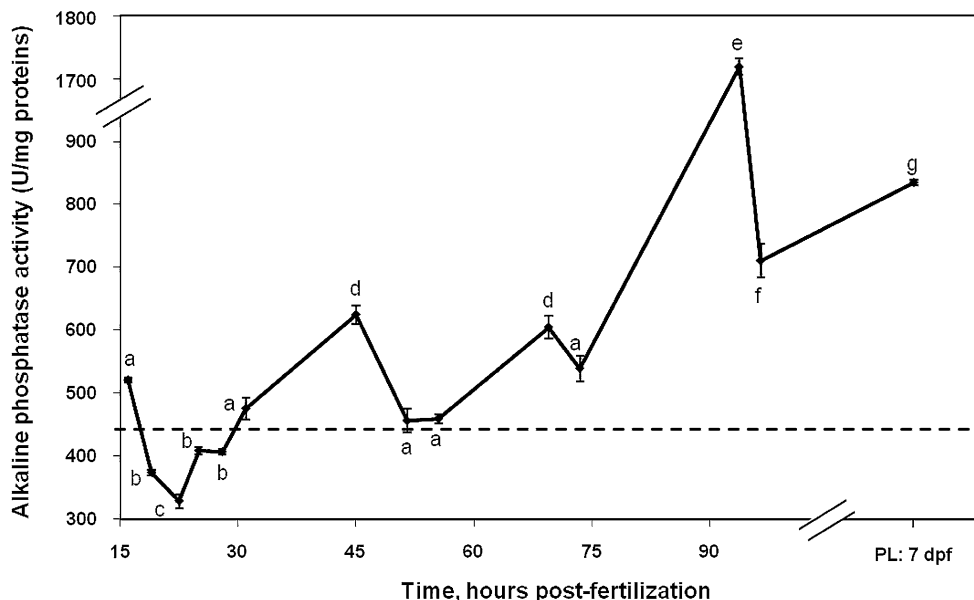


**Fig. 5** Carbonic anhydrase activity in adult abalone tissues and effect of acetazolamide. Carbonic anhydrase activity was measured in mantle and gills of 7-cm-length abalone dissected in March. Data represent the mean ± s.e.m. of 5 animals. The human carbonic anhydrase II (hCA) activity was also measured at a concentration of 1 µg/ml as a positive control, and data represent the mean ± s.e.m. of

4 values. The activity is expressed in Units per mg of total proteins for hCA and in milliUnits per mg of total proteins for tissues. A specific inhibitor, the acetazolamide (AZ, 30 µM) was used to verify the specificity of the method. The difference was significant with *P* < 0.01

**Fig. 6** Carbonic anhydrase activity during larval development. Each point represents the mean  $\pm$  s.e.m. of four values. The experiment was carried out 3 times on a same pool of about 15,000 larvae collected in 2008, and the same trend was observed each time. A similar trend was observed for larvae collected in 2007 and 2006. CA activity measured in mantle of a 7-cm-abalone is reported in *dotted line*. Results are expressed in milliUnits of activity per mg of total proteins in each larval extract. The *letters*, when different, indicate a significant difference between stages ( $P < 0.05$ ). dpf: days post-fertilization

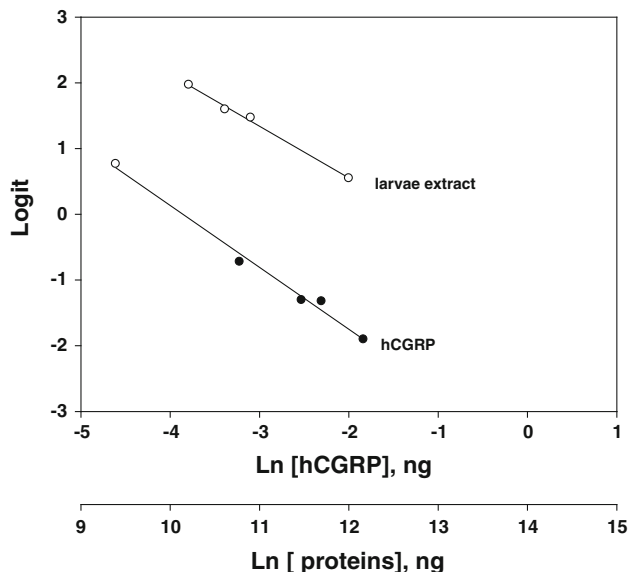
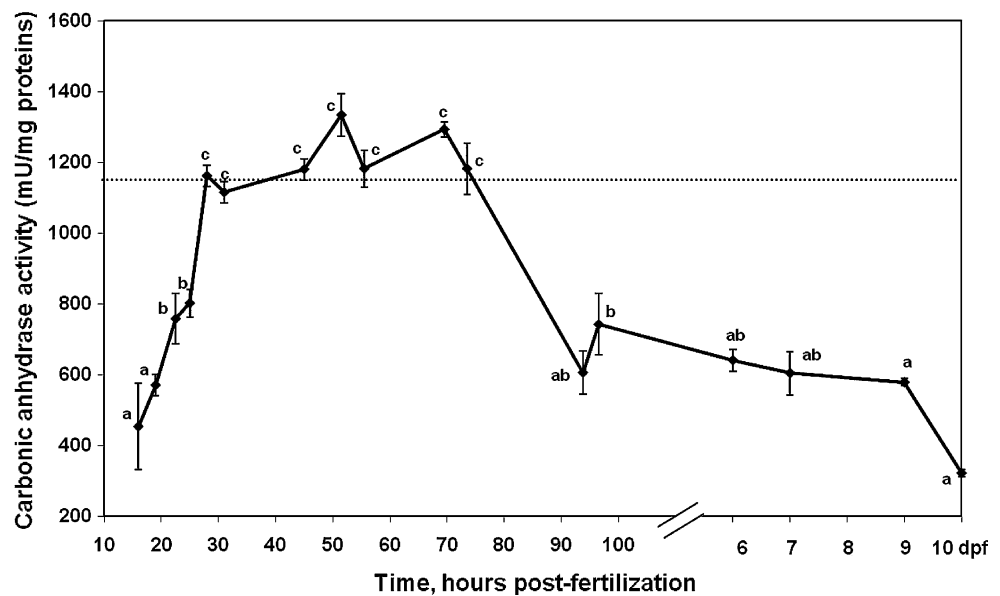


**Fig. 7** Effect of standard human CGRP and larval extracts on the binding of  $^{125}\text{I}$ -CGRP to the anti-human CGRP antibody. Immunoreactive CGRP-like molecules were quantified with a specific radioimmunoassay using five dilutions from hCGRP and four dilutions from larval extracts (31 hpf). The logit transformation ( $\ln[(B/B_0)/(1-(B/B_0))]$ ) of the percentage of initial binding of  $^{125}\text{I}$ -CGRP ( $B/B_0 \times 100$ ) was plotted as a function of Ln of protein/peptide concentration. Correlation coefficient lines were  $r^2 = 0.9901$  for human CGRP and  $r^2 = 0.9952$  for larval extracts

larval development, corresponding to the formation of protoconch I, the activity increases exponentially and reaches its maximum around larval torsion. CA activity remains at a high level until the achievement of protoconch II and dramatically decreases before metamorphosis (Fig. 9). This succession of CA activation/inhibition observed during abalone shell formation is

consistent with a previous study on bivalve shell formation that correlated CA activity variations with the main steps of shell morphogenesis (Medakovic 2000). The enhancement of CA activity during active growth of abalone protoconch confirms the involvement of CA in the rapid shell growth of mollusks (Freeman 1960; Medakovic 2000; Wilbur and Jodrey 1956). The most obvious role of this enzyme would be the enhancement of bicarbonate ion formation when rapid  $\text{CaCO}_3$  precipitation is required. Furthermore, a matrix protein, called nacrein, was identified in the nacreous layer of *Pinctada fucata* and *Turbo marmoratus* (Miyamoto et al. 1996; Miyamoto et al. 2003). This protein, characterized by two carbonic anhydrase domains, is known to act in aragonite crystal formation (Miyamoto et al. 1996). Since the first mineral phase deposited in larval abalone shell is aragonite, CA activity may partly come from a nacrein-like protein. Experiments are underway to identify a nacrein-like protein in abalone.

The succession of enzymatic activation and inhibition events throughout the larval development of *H. tuberculata* strongly suggests a physiologic control of calcification. The presence and the role of CGRP in mollusks were previously investigated to understand the regulation of calcium metabolism during shell growth (Auzoux-Bordenave et al. 2007; Duvail and Fouchereau-Peron 2001; Duvail et al. 1997; 1999; Rousseau et al. 2003). The variations of CGRP-like molecules in biomineralizing tissues as well as in circulating hemolymph may well correspond to an endocrine/paracrine system controlling the biomineralization process in adult mollusks. In the present study, the level of CGRP-related molecules varied along the development cycle of the abalone (Fig. 9). At larval stages, the level is close to that found in the adult mantle at the end of

**Fig. 8** Larval and post-larval CGRP-like immunoreactivity as a function of developmental stage. CGRP-like molecules (ir-CGRP) in larvae were quantified using a human CGRP radioimmunoassay, in each experimental group. Each point represents the mean  $\pm$  s.e.m. of three values. Results are expressed as pg immunoreactive related molecules per mg of total proteins in each larval extract. Each assay was performed in triplicate. The *asterisks* indicate a significant difference between larval and post-larval stages ( $P < 0.01$ )

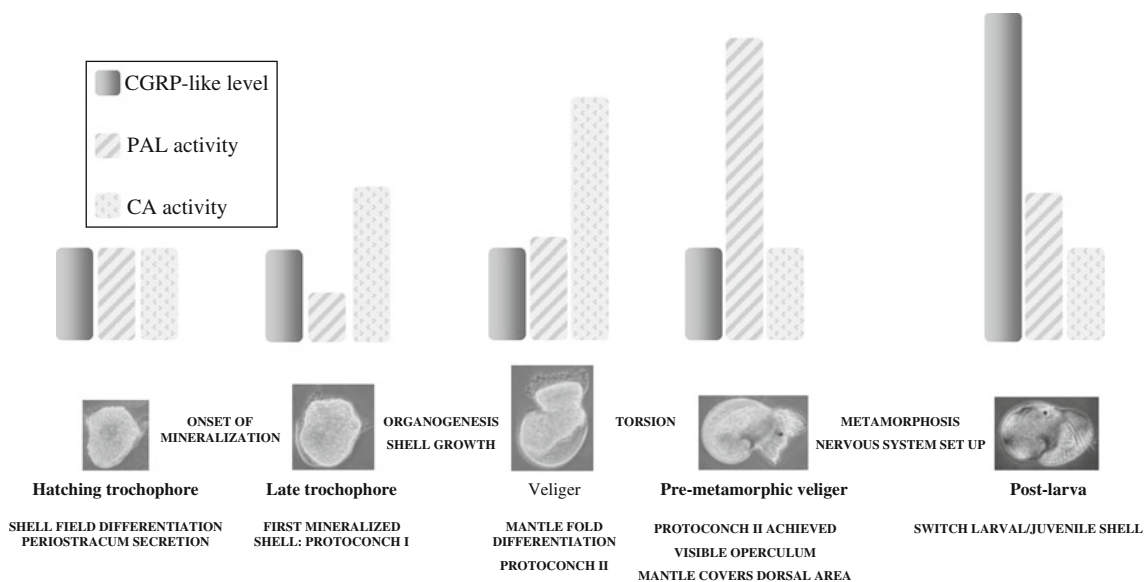
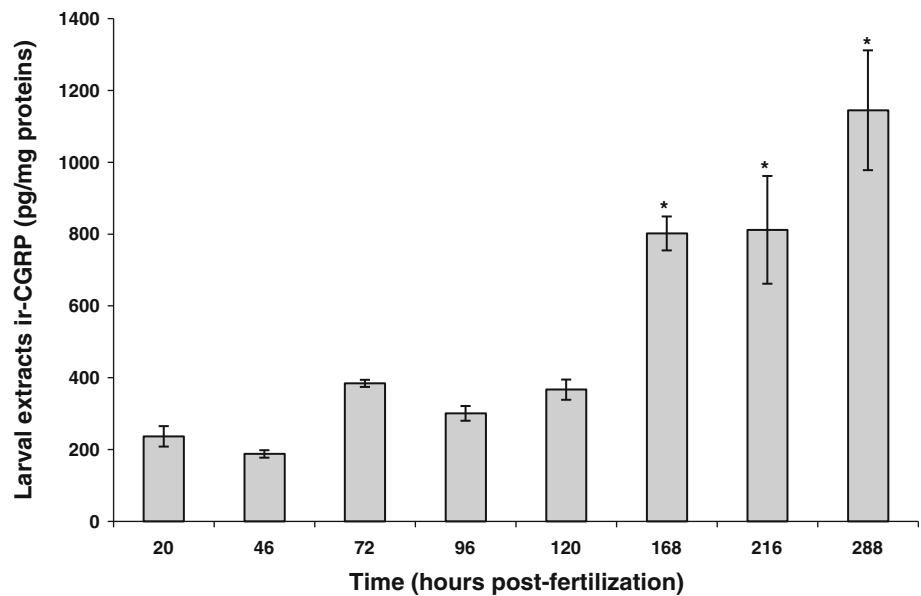


**Fig. 9** Schematic drawing showing variations of enzymatic activities and CGRP-like molecules level related to the shell formation events. Alkaline phosphatase activity is higher when the shell field and then the periostracum set up and before the transition of protoconch-to-juvenile shell. CA activity exponentially increases during active

growth of the protoconch, from hatching to torsion event and remains high until the achievement of protoconch. After the set up of nervous system during metamorphosis, CGRP-like molecules strongly increase in post-larvae

shell growth (Duvail and Fouchereau-Peron 2001). In seven-day-old post-larvae, at the transition between larval and juvenile shell, the level of CGRP-like molecule peaks, reaching 3 times the mean level assessed before metamorphosis. The concentration of CGRP-like molecules in post-larvae is comparable to that found in abalone mantle during active shell growth (Duvail and Fouchereau-Peron 2001). Thus, the highest concentrations of immunoreactive CGRP molecules are found between post-larval and juvenile stages, a period corresponding to the optimal shell

growth (Basuyaux 1997). These findings clearly suggest the post-metamorphic establishment of an endocrine control of the calcium metabolism. Indeed, the nervous system sets up gradually during metamorphosis with the progressive establishment of nervous connections (Crofts 1937). This could correspond to the onset of CGRP-like molecules secretion in post-larvae. Further Radio-receptor assays and  $^{45}\text{Ca}$  incorporation experiments are needed to define the target organs of this neuropeptide in abalone and confirm its hypocalcemic role.

This work brings new insight into the enzymatic and endocrine control of shell mineralization in the European abalone *Haliotis tuberculata*. To clarify the molecular and cellular mechanisms involved in shell mineralization, further studies of the organic/mineral interface would be essential. Current investigations on organic matrix molecules combined with high-resolution analysis will contribute significantly to the understanding of the biomineralization sequence throughout the molluscan development cycle.

**Acknowledgments** We thank B. Marie, F. Marin (University of Bourgogne, Dijon, France), C. Milet (Muséum National d'Histoire Naturelle, Paris, France), and J.-Y. Sire (University of Paris 6) for helpful discussions. We also thank S. Thompson (University of Keele, UK) for the English corrections. FTIR analyses were carried out at the Muséum National d'Histoire Naturelle; we thank Pr. F. Fröhlich (MNHN) for help in FTIR spectra interpretation. This work was supported in part by the European Community: The Atlantic Area Programme BIOTECMAR n° 2008-1/032 and by the Programme PluriFormations "Biominalization". B. Gaume was financed by a PhD fellowship from the Ministère de l'Enseignement Supérieur et de la Recherche, in France. The experiments complied with the current French laws.

## References

- Almeida MJ, Milet C, Peduzzi J, Pereira L, Haigle J, Barthélemy M, Lopez E (2000) Effect of water-soluble matrix fraction extracted from the nacre of *Pinctada maxima* on the alkaline phosphatase activity of cultured fibroblasts. *J Exp Zool Part B Mol Dev Evol* 288:327–334. doi:10.1002/1097-010X(20001215)288:4<327::AID-JEZ5>3.0.CO;2-#
- Amara SG, Jonas V, Rosenfeld MG, Ong ES, Evans RM (1982) Alternative RNA processing in calcitonin gene expression generates mRNAs encoding different polypeptide products. *Nature* 298:240–244. doi:10.1038/298240a0
- Auzoux-Bordenave S, Fouchereau-Peron M, Helléouet M-N, Doumenc D (2007) CGRP regulates the activity of mantle cells and hemocytes in abalone primary cell cultures (*Haliotis tuberculata*). *J Shellfish Res* 26:887–894. doi:10.2983/0730-8000(2007)26[887:CRTAOM]2.0.CO;2
- Basuyaux O (1997) Etude et modélisation des paramètres physico-chimiques sur la croissance de l'ormeau (*Haliotis tuberculata*) en élevage en circuit semi-fermé. Thèse de Doctorat, Spécialité: Sciences, Université de Caen, France
- Belcher AM, Wu XH, Christensen RJ, Hansma PK, Stucky GD, Morse DE (1996) Control of crystal phase switching and orientation by soluble mollusc-shell proteins. *Nature* 381:56–58. doi:10.1038/381056a0
- Bevelander G (1988) Development. In: Bevelander G (ed) Abalone: gross and fine structure. The Boxwood Press, Pacific Groove, p 2
- Bevelander G, Benzer P (1948) Calcification in marine molluscs. *Biol Bull* 94:176–183
- Bielefeld U, Becker W (1991) Embryonic development of the shell in *Biomphalaria glabrata* (Say). *Int J Dev Biol* 35:121–131
- Blasco J, Puppo J, Sarasquete MC (1993) Acid and alkaline phosphatase activities in the clam *Ruditapes decussatus*. *Mar Biol* 115:113–118. doi:10.1007/BF00349392
- Bourgoin SG, Harbour D, Poubelle PE (1996) Role of protein kinase C alpha, Arf, and cytoplasmic calcium transients in phospholipase D activation by sodium fluoride in osteoblast-like cells. *J Bone Miner Res* 11:1655–1665. doi:10.1002/jbmr.5650111109
- Crofts DR (1937) The development of *Haliotis tuberculata*, with special reference to organogenesis during torsion. *Philos Trans R Soc Lond B Biol Sci* 228:219–268. doi:10.1098/rstb.1937.0012
- Cudennec B, Rousseau M, Lopez E, Fouchereau-Peron M (2006) CGRP stimulates gill carbonic anhydrase activity in molluscs via a common CT/CGRP receptor. *Peptides* 27:2678–2682. doi:10.1016/j.peptides.2006.05.019
- Dauphin Y, Cuif J-P, Mutvei H, Denis A (1989) Mineralogy, chemistry and ultrastructure of the external shell-layer in ten species of *Haliotis* with reference to *Haliotis tuberculata* (Mollusca: Archaeogastropoda). *Bull Geol Inst Univ Uppsala NS* 15:7–38
- Duvail L, Fouchereau-Peron M (2001) Calcium metabolism related markers during the growth of *Haliotis tuberculata*. *Invertebr Reprod Dev* 40:209–216
- Duvail L, Lopez E, Fouchereau-Peron M (1997) Characterization of a calcitonin gene related peptide-like molecule in the abalone, *Haliotis tuberculata*. *Comp Biochem Physiol C Pharmacol Toxicol Endocrinol* 116:155–159. doi:10.1016/S0742-8413(96)00193-4
- Duvail L, Lopez E, Fouchereau-Peron M (1999) Characterization of binding sites for calcitonin gene related peptide in abalone gill. *Peptides* 20:361–366. doi:10.1016/S0196-9781(99)00043-1
- Falini G, Albeck S, Weiner S, Addadi L (1996) Control of aragonite or calcite polymorphism by mollusk shell macromolecules. *Science* 271:67–69. doi:10.1126/science.271.5245.67
- Fouchereau-Peron M (1993) Characterization of a molecule related to calcitonin gene-related peptide (CGRP) in the scallop, *Pecten maximus*. *Comp Biochem Physiol B Biochem Mol Biol* 105:707–711. doi:10.1016/0305-0491(93)90109-I
- Freeman JA (1960) Influence of carbonic anhydrase inhibitors on shell growth of a fresh-water snail, *Physa heterostropha*. *Biol Bull* 118:412–418
- Freeman JA, Wilbur KM (1948) Carbonic anhydrase in molluscs. *Biol Bull* 94:55–59
- Fröhlich F, Gendron-Badou A (2002) La spectroscopie infrarouge, un outil polyvalent. In: Miskovsky J-C (ed) Géologie de la Préhistoire. AEEGP, éditeur, Paris, pp 662–677
- Genge BR, Sauer GR, Wu LNY, McLeane FM, Wuthier RE (1988) Correlation between loss of alkaline phosphatase activity and accumulation of calcium during matrix vesicle-mediated mineralization. *J Biol Chem* 263:18513–18519
- Jablonski B, Lutz RA (1980) Molluscan larval shell morphology, ecological and paleontological applications. In: Rhoads DC, Lutz RA (eds) Skeletal growth of aquatic organisms. Plenum Press, New York, pp 323–377
- Jackson D, Worheide G, Degnan B (2007) Dynamic expression of ancient and novel molluscan shell genes during ecological transitions. *BMC Evol Biol* 7:160. doi:10.1186/1471-2148-7-160
- Jardillier E, Rousseau M, Gendron-Badou A, Fröhlich F, Smith D, Martin M, Helléouet M-N, Huchette S, Doumenc D, Auzoux-Bordenave S (2008) A morphological and structural study of the larval shell from the abalone *Haliotis tuberculata*. *Mar Biol* 154:735–744. doi:10.1007/s00227-008-0966-3
- Joesse J (1988) The hormones of molluscs. In: Laufer H (ed) Endocrinology of selected invertebrate types. Alan R Liss, New York, pp 89–140
- Kniprath E (1981) Ontogeny of the molluscan shell field: a review. *Zool Scr* 10:61–79. doi:10.1111/j.1463-6409.1981.tb00485.x
- Lau KH, Farley JR, Baylink DJ (1985) Phosphotyrosyl-specific protein phosphatase activity of a bovine skeletal acid phosphatase isoenzyme. Comparison with the phosphotyrosyl protein phosphatase activity of skeletal alkaline phosphatase. *J Biol Chem* 260:4653–4660

- Levi-Kalisman Y, Falini G, Addadi L, Weiner S (2001) Structure of the nacreous organic matrix of a bivalve mollusk shell examined in the hydrated state using cryo-TEM. *J Struct Biol* 135:8–17. doi:[10.1006/jbsi.2001.4372](https://doi.org/10.1006/jbsi.2001.4372)
- Lin A, Meyers MA (2005) Growth and structure in abalone shell. *Mater Sci Eng A* 390:27–41. doi:[10.1016/j.msea.2004.06.072](https://doi.org/10.1016/j.msea.2004.06.072)
- Lowenstam HA, Weiner S (1989) On biomineralization. Oxford University Press, New York
- Marin F, Luquet G (2004) Molluscan shell proteins. *CR Palevol* 3:469–492. doi:[10.1016/j.crpv.2004.07.009](https://doi.org/10.1016/j.crpv.2004.07.009)
- Marin F, Luquet G, Marie B, Medakovic D, Gerald PS (2007) Molluscan shell proteins: primary structure, origin, and evolution. *Curr Top Dev Biol* 80:209–276. doi:[10.1016/S0070-2153\(07\)80006-8](https://doi.org/10.1016/S0070-2153(07)80006-8)
- Martoja R, Martoja M (1967) Initiation aux techniques de l'histologie animale. Masson et Cie, Paris
- Marxen JC, Witten PE, Finke D, Reelsen O, Rezgaoui M, Becker W (2003) A light- and electron-microscopic study of enzymes in the embryonic shell-forming tissue of the freshwater snail, *Biomphalaria glabrata*. *Invertebr Biol* 122:313–325. doi:[10.1111/j.1744-7410.2003.tb00096.x](https://doi.org/10.1111/j.1744-7410.2003.tb00096.x)
- Medakovic D (2000) Carbonic anhydrase activity and biomineralization process in embryos, larvae and adult blue mussels *Mytilus edulis* L. *Helgol Mar Res* 54:1–6. doi:[10.1007/s101520050030](https://doi.org/10.1007/s101520050030)
- Miyamoto H, Miyashita T, Okushima M, Nakano S, Morita T, Matsushiro A (1996) A carbonic anhydrase from the nacreous layer in oyster pearls. *Proc Natl Acad Sci USA* 93:9657–9660. doi:[10.1073/pnas.93.18.9657](https://doi.org/10.1073/pnas.93.18.9657)
- Miyamoto H, Yano M, Miyashita T (2003) Similarities in the structure of nacrein, the shell-matrix protein, in a bivalve and a gastropod. *J Molluscan Stud* 69:87–89
- Mutvei H, Dauphin Y, Cuif J-P (1985) Observations sur l'organisation de la couche externe du test des *Haliotis* (Gastropoda): un cas exceptionnel de la variabilité minéralogique et microstructurale. *Bull Mus natn His nat Paris*, 4e ser, 7: 73–91
- Page LR (1997) Ontogenetic torsion and protoconch form in the archaeogastropod *Haliotis kamschatkana*: evolutionary implications. *Acta Zool* 78:227–245. doi:[10.1111/j.1463-6395.1997.tb01009.x](https://doi.org/10.1111/j.1463-6395.1997.tb01009.x)
- Pichard C, Fröhlich F (1986) Analyses infrarouges quantitatives des sédiments. Exemple du dosage du quartz et de la calcite. *Rev Inst Fr Pétrrol* 41:809–819
- Rousseau M, Plouguerne E, Wan G, Wan R, Lopez E, Fouchereau-Peron M (2003) Biomineralisation markers during a phase of active growth in *Pinctada margaritifera*. *Comp Biochem Physiol A Mol Integr Physiol* 135:271–278. doi:[10.1016/S1095-6433\(03\)00070-9](https://doi.org/10.1016/S1095-6433(03)00070-9)
- Timmermans LPM (1969) Studies on shell formation in molluscs. *Neth J Zool* 19:417–523
- Tippins JR, Morris HR, Panico M, Etienne T, Bevis P, Girgis S, MacIntyre I, Azria M, Attinger M (1984) The myotropic and plasma-calcium modulating effects of calcitonin gene-related peptide (CGRP). *Neuropeptides* 4:425–434. doi:[10.1016/0143-4179\(84\)90118-5](https://doi.org/10.1016/0143-4179(84)90118-5)
- Tsujii T (1976) An electron microscopic study of the mantle cells of *Anodonta* sp. during shell regeneration. In: Watabe N, Wilbur KM (eds) The mechanisms of mineralization in the invertebrates and plants. University of South Carolina Press, Columbia, pp 339–353
- Vignery A, McCarthy TL (1996) The neuropeptide calcitonin gene-related peptide stimulates insulin-like growth factor I production by primary fetal rat osteoblasts. *Bone* 18:331–335
- Vitale AM, Monserrat JM, Castilho P, Rodriguez EM (1999) Inhibitory effects of cadmium on carbonic anhydrase activity and ionic regulation of the estuarine crab *Chasmagnathus granulata* (Decapoda, Grapsidae). *Comp Biochem Physiol C Pharmacol Toxicol Endocrinol* 122:121–129. doi:[10.1016/S0742-8413\(98\)10094-4](https://doi.org/10.1016/S0742-8413(98)10094-4)
- Watabe N (1988) Shell structure. In: The Mollusca, vol 11. Academic Press, New York, pp. 69–104
- Weiss IM, Marin F (2008) The role of enzymes in biomineralization processes. *Met. Ions Life Sci.* In: Sigel A, Sigel H, Sigel RKO (eds) “Biomineralization. From Nature to Application” vol 4, Wiley, Chichester, England, pp. 71–126
- Wilbur KM, Jodrey LH (1956) Studies on shell formation V. The inhibition of shell formation by carbonic anhydrase inhibitors. *Biol Bull* 108:359–365
- Wilbur KM, Saleuddin ASM (1983) Shell formation. In: The Mollusca, vol 4. Academic Press, New York, pp 235–285